

Breakdown of the Stokes-Einstein Relation in Supercooled Water

Pradeep Kumar¹, S. V. Buldyrev², S. R. Becker,³
P. H. Poole⁴, F. W. Starr³, and H. E. Stanley¹

¹Center for Polymer Studies and Department of Physics, Boston University, Boston, MA 02215 USA

²Yeshiva University, Department of Physics, 500 West 185th Street, New York, New York 10033, USA

³Department of Physics, Wesleyan University, Middletown, CT 06459, USA

⁴Department of Physics, St. Francis Xavier University, Antigonish, Nova Scotia B2G 2W5, Canada

PACS: 05.40.-a

REVISED: 09 Jan

ABSTRACT

Supercooled water exhibits a breakdown of the Stokes-Einstein relation between the diffusion constant D and the alpha relaxation time τ_α . For water simulated with the TIP5P and ST2 potentials, we find that the temperature of the decoupling of diffusion and alpha relaxation correlates with the temperature of the maximum in specific heat that corresponds to crossing the Widom line $T_W(P)$. Specifically, we find that our results for $D\tau_\alpha/T$ collapse onto a single master curve if temperature is replaced by $T - T_W(P)$, where $T_W(P)$ is the temperature where the constant-pressure specific heat achieves a maximum. Also, we find agreement between our ST2 simulations and experimental values of $D\tau_\alpha/T$. We further find that the size of the mobile molecule clusters (dynamical heterogeneities) increases sharply near $T_W(P)$. Moreover, our calculations of mobile particle cluster size $\langle n(t^*) \rangle_w$ for different pressures, where t^* is the time for which the mobile particle cluster size is largest, also collapse onto a single master curve if T is replaced by $T - T_W(P)$. The crossover to a more locally structured low density liquid (LDL) environment as $T \rightarrow T_W(P)$ appears to be well correlated with both the breakdown of the Stokes-Einstein relation and the growth of dynamic heterogeneities.

A 17th century study of the density maximum at 4°C [1] demonstrates the long history of water science [2, 3, 4, 5]. Since that time, dozens of additional anomalies of water have

been discovered [6], including the sharp increase upon cooling of both the constant-pressure specific heat C_P and the isothermal compressibility K_T . These anomalies of water become more pronounced as water is supercooled. To explain these properties, a liquid-liquid (LL) critical point has been proposed [7]. Emanating from this critical point there must be loci of extrema of thermodynamic response functions such as C_P and K_T . These loci must coincide as the critical point is approached, since response functions are proportional to powers of the correlation length, and the locus of the correlation length maxima asymptotically close to the critical point defines the Widom line.

In the supercooled region of the pressure-temperature phase diagram, the dynamic properties of water show dramatic changes [8, 9]. One basic relation among dynamic properties is the Stokes-Einstein (SE) relation

$$D = \frac{k_B T}{6\pi\eta a}, \quad (1)$$

where D is the diffusion constant, T is the temperature, k_B is the Boltzmann constant, η is the viscosity and a is the effective hydrodynamic radius of a molecule. This expression provides a relation between mass and momentum transport of a spherical object in a viscous medium. The SE relation describes nearly all fluids at $T \gtrsim 1.2 - 1.6 T_g$, where T_g is the glass transition temperature, and since the hydrodynamic radius a is roughly constant, $D\eta/T$ is approximately independent of T [10, 11, 12]. However, in most liquids, for $T \lesssim 1.2 - 1.6 T_g$ $D\eta/T$ is no longer a constant [13, 13, 14, 15, 16, 17, 18, 19, 20, 21, 22]. For the case of water, the breakdown of the SE relation occurs about $1.8T_g$, in the same temperature region in which many of the unusual thermodynamic features of water occur [5, 8, 23].

Our aim is to evaluate to what degree the SE breakdown can be correlated with the presence of thermodynamic anomalies and the onset of spatially heterogeneous dynamics, and how these features relate to the location of the Widom line [16, 24, 25, 26, 27]. From prior studies of water, we can already form an expectation for the correlation between the SE breakdown and the Widom line by combining three elements: (i) the Widom line is approximately known from the extrapolated power-law divergence of K_T [28]; (ii) the locus of points $T_D(P)$ where D extrapolates to zero is also known, and nearly coincides with $T_W(P)$ at low pressures (see Fig.1 of Ref. [29]); (iii) the SE relation has been found to fail in liquids generally at the temperature $T_D(P)$ [30]. Combining these three results, one might not be surprised if the breakdown of the SE relation should occur near to the Widom

line for $P < P_C$, and it should continue to follow $T_D(P)$ for $P > P_C$. We will see that our results are consistent with this expectation, but reveal some unexpected insights. To address these issues, we perform molecular dynamics (MD) simulations of $N = 512$ waterlike molecules interacting via the TIP5P potential [31, 32], which exhibits a LL critical point at approximately $T_C \approx 217$ K and $P_C \approx 340$ MPa [32, 33]. We carry out simulations in the NPT ensemble for three different pressures $P = 0$ MPa, 100 MPa, and 200 MPa, and for temperatures T ranging from 320 K down to 230 K for $P = 0$ and 100 MPa, and down to 220 K for 200 MPa. We also analyze MD simulations of $N = 1728$ waterlike molecules interacting via the ST2 potential [34, 35], which displays a LL critical point at $T_C \approx 245$ K and $P = 180$ MPa [36]. The simulations for the ST2 model are performed in the NVT ensemble [35]. To locate the Widom line, we first analyze the isobaric heat capacity C_P for the TIP5P model [Fig. 1(a)]. For the ST2 model, we use the results for the Widom line from Ref. [36].

We next explore the possible relation between the Widom line and the breakdown of the SE relation (Eq. 1). We first calculate the diffusion constant via its asymptotic relation to the mean-squared displacement,

$$D \equiv \lim_{t \rightarrow \infty} \frac{\langle |\mathbf{r}_j(t) - \mathbf{r}_j(0)|^2 \rangle}{6t}, \quad (2)$$

where $\mathbf{r}_j(t)$ is the position of oxygen j at time t . It is difficult to accurately calculate the viscosity η in simulations, so we instead calculate the alpha relaxation time τ_α (which is expected to have nearly the same T dependence as η) as the time at which the coherent intermediate scattering function

$$F(q, t) \equiv \frac{\langle \rho(\mathbf{q}, t) \rho(-\mathbf{q}, 0) \rangle}{\langle \rho(\mathbf{q}, 0) \rho(-\mathbf{q}, 0) \rangle}, \quad (3)$$

decays by a factor of e . Here $\rho(\mathbf{q}, t) \equiv \sum_j^N \exp[-i\mathbf{q} \cdot \mathbf{r}_j(t)]$ is the Fourier transform of the density at time t , $\mathbf{r}_j(t)$ is the position of oxygen j at time t , \mathbf{q} is a wave vector and the brackets denote an average over all $|\mathbf{q}| = q$ and many equilibrium starting configurations. We calculate $F(q, t)$ at the value of q of the first maximum in the static structure factor $F(q, 0)$. It is important that we use the coherent scattering function (as opposed to the incoherent, or self-scattering function), since we want to capture collective relaxation that contributes to η . Hence the SE relation can be written as

$$\frac{D\tau_\alpha}{T} = \text{constant}. \quad (4)$$

We see that both τ_α and D (Fig. 1(b)) display rapid changes at low T .

Figures 2(a) and 2(b) show $D\tau_\alpha/T$ as a function of T . At high T , $D\tau_\alpha/T$ remains approximately constant. At low T , $D\tau_\alpha/T$ increases indicating a breakdown of the SE relation (1), which occurs in the same T region where the thermodynamic anomalies develop, and near the Widom line $T_W(P)$. To test if there is a correlation between the SE breakdown and $T_W(P)$, we plot $D\tau_\alpha/T$ against $T - T_W(P)$ [Figs. 2(c) and (d)] and find the unexpected result that all the curves for different pressures overlap within the limits of our accuracy for both TIP5P and ST2 potentials. Hence $D\tau_\alpha$ is a function only of $T - T_W(P)$, from which it follows that the locus of the temperature of the breakdown of the SE relation is correlated with $T_W(P)$.

To better quantify the temperature where the SE relation breaks down, we use the fact that when the SE relation fails it can be replaced by a “fractional” SE relation $D(\tau_\alpha/T)^\xi = \text{const}$ [13, 35]. By plotting parametrically $\log(D)$ as a function of $\log(\tau_\alpha/T)$, one can identify the crossover temperature $T_\times(P)$ between the two regions by the intersection of the high T SE behavior and the low T fractional SE behavior [Fig. 3]. We confirm that the same collapse of $D\tau_\alpha/T$ can be found by replacing T with $T - T_\times(P)$, demonstrating (Fig. 3) that the loci of SE breakdown defined by $T_\times(P)$ and $T_W(P)$ track each other for $P < P_C$. There is also some difference between the ST2 and TIP5P models in the relative location of the breakdown of the SE relation and $T_W(P)$, evidenced by the fact that the magnitude of the SE breakdown is different at $T = T_W(P)$. As a result, the data for the two models will not collapse when plotted together. Moreover, we find that $D\eta/T$ from the experimental data plotted against $T - T_W(P)$ [Fig. 2(d)], coincides with the ST2 results, suggesting that the data collapse should exist for real water when T is replaced by $T - T_W(P)$ [37, 38].

The above analysis has primarily focused on the behavior for $P < P_C$, where there is a Widom line. For $P > P_C$, water behaves similarly to simple glass forming liquids, and we expect the breakdown of the SE relation for water to be similar to other simple liquids. Specifically, the SE relation should break down at $T \approx 1.2 - 1.6T_g$ [13]. This breakdown approximately coincides with the temperature where the mode coupling description of the dynamics fails [13, 30]. For the SPC/E model of water, the mode coupling temperature ($T_{MCT}(P)$) locus has been evaluated, and the slope in the P - T plane of this locus changes from negative to positive for $P > P_C$ [39] (the slope is positive for simple liquids). Correspondingly, there is also a decoupling of D and τ_α near $T_{MCT}(P)$ [39]. We find the same

behavior for the ST2 model.

Since we find a correlation between $T_W(P)$ and the breakdown of the SE relation, the hypothesized connection between the SE breakdown and the onset of dynamical heterogeneities (DH) suggests a connection between $T_W(P)$ and the onset of DH. To investigate the behavior of the dynamic heterogeneities, we study the clusters formed by the 7% most mobile molecules [40], defined as molecules with the largest displacements during a certain interval of time of length t . The clusters of the most mobile molecules are defined as follows. If in a pair of the most mobile molecules determined in the interval $[t_0, t_0 + t]$, two oxygens at time t_0 are separated by less than the distance corresponding to position of the first minimum in the pair correlation function (0.315 nm in TIP5P and 0.350 nm in ST2), this pair belongs to the same cluster.

The weight averaged mean cluster size

$$\langle n(t) \rangle_w \equiv \frac{\langle n^2(t) \rangle}{\langle n(t) \rangle}, \quad (5)$$

measures the cluster size to which a randomly chosen molecule belongs, where $\langle n(t) \rangle$ is the number averaged mean cluster size. We show $\langle n(t) \rangle_w$ in Fig. 4 for TIP5P as a function of observation time interval t for different T at $P = 0$ MPa [Fig. 4(a)]. The behavior at higher P is qualitatively the same [Fig. 4(b)]. At low T , $\langle n(t) \rangle_w$ has a maximum at the time t^* associated with the breaking of the cage formed by the neighboring molecules (see [41] and the references therein). Both the magnitude and the time scale t^* of the peak grow as T decreases. At high T , this peak merges and becomes indistinguishable from a second peak with fixed characteristic time ≈ 0.5 ps. By evaluating the vibrational density of states, we associate this feature with a low frequency vibrational motion of the system, probably the O-O-O bending mode [42].

To probe the temperature dependence of $\langle n(t) \rangle_w$, we plot the peak value $\langle n(t^*) \rangle_w$ in Fig. 4(c) as a function of T for $P = 0$ MPa, 100 MPa, and 200 MPa for the TIP5P model. At high T , $\langle n(t^*) \rangle_w$ is nearly constant, since at high T , clusters result simply from random motion of the molecules. Upon cooling near the Widom line, $\langle n(t^*) \rangle_w$ increases sharply. When $\langle n(t^*) \rangle_w$ is plotted as a function of $T - T_W(P)$ [see Fig. 4(d)], we find that (similarly to the behavior of $D\tau_\alpha/T$) the three curves for $P = 0$ MPa, $P = 100$ MPa, and $P = 200$ MPa overlap, and it is apparent that the pronounced increase in $\langle n(t^*) \rangle_w$ occurs for $T \approx T_W(P)$.

To further test that the breakdown of the SE relation in water is associated with the

onset of large DH near the Widom line, we show $\langle n(t) \rangle_w$ for different T along an isochore of density $\rho = 0.83 \text{ g/cm}^3$ for the ST2 model of water in Fig. 5(a). We show an isochore because only isochoric data are available from Ref. [36]. As in the case of TIP5P, we find the emergence of a second time scale larger than 0.5 ps in $\langle n(t) \rangle_w$ near the crossing of the Widom line at this density. Similarly, $\langle n(t^*) \rangle_w$ increases sharply near the Widom line temperature [see Fig. 5(b)]. Hence the sharp growth of DH and the appearance of a second time scale in $\langle n(t) \rangle_w$ both occur near the Widom line. We also find that the magnitude of $\langle n(t^*) \rangle_w$ is larger for the ST2 model than for the TIP5P model at the Widom temperature, consistent with the above observation that the breakdown of the SE relation is more pronounced for the ST2 model than for the TIP5P model.

Finally, we consider the correspondence between DH and static structural heterogeneity in the supercritical region; this region is characterized by large fluctuations spanning a wide range of structures, from HDL-like to LDL-like. To quantify these structural fluctuations, we calculate for the TIP5P model the temperature derivative of a local tetrahedral order parameter Q [43]. In Fig. 6(a), we show $|(\partial Q/\partial T)_P|$ at different T for $P = 0 \text{ MPa}$, and 100 MPa, and find maxima [44] at $T_W(P)$ [45, 46]. The maxima in $|(\partial Q/\partial T)_P|$ indicates that the change in local tetrahedrality is maximal at $T_W(P)$, which should occur when the structural fluctuation of LDL-like and HDL-like components is largest. We see that the growth of the dynamic heterogeneity coincides with the maximum in fluctuation of the local environment. Also, since Q quantifies the orientational order, the fact that we find that $|(\partial Q/\partial T)_P|$ has maximum at approximately the same temperature where $C_P = T(\partial S/\partial T)_P$ has a maximum, supports the idea that water anomalies are closely related to the orientational order present in water.

Before concluding, we note that more than a dozen other phenomena have been correlated with $T_W(P)$. Some of these phenomena are from simulations, such as the crossover in the relaxation time of the fluctuations in orientational order parameter Q [47] or the maximum in the temperature derivative of the number of hydrogen bonds per molecule [48]. Others are from only experiments, such as the sharp drop in the the temperature derivative of the zero-frequency structure factor observed by QENS or the appearance of a Boson peak, both observed by quasi-elastic neutron scattering [49]. Finally, some anomalies that correlate with the Widom line are found in both simulations and experiment, such as the dynamic “fragile-to-strong” crossover in the diffusion constant, or the sharp drop in temperature

derivative of the mean squared displacement (seen in QENS, NMR, and simulations) [44, 45, 50].

In conclusion, we find that the breakdown of the Stokes-Einstein relation for $P < P_C$ can be correlated with the Widom line. In particular, rescaling T by $T - T_W(P)$ yields good data collapse of $D\tau_\alpha/T$ for different pressures. Rapid structural changes occur at T near the Widom line, where larger LDL “patches” emerge upon cooling. The size of the dynamic heterogeneities also increases sharply as the Widom line is crossed. The breakdown of the SE relation can be understood by the fact that diffusion at low T is dominated by regions of fastest moving molecules (DH) while the relaxation of the system as a whole is dominated by slowest moving molecules. Consistent with this, we found that the growth of mobile particle clusters occurs near the Widom line and also near the breakdown of the SE relation for $P < P_C$. Thus the SE breakdown in water is consistent with the LL-critical point hypothesis [2, 3, 4, 5, 7]. Our results are also consistent with recent experimental findings in confined water [8, 49, 50].

We thank C. A. Angell, S.-H. Chen, G. Franzese, J. M. H. Levelt Sengers, S. Han, L. Liu, M. G. Mazza, F. Sciortino, M. Sperl, K. Stokely, B. Widom, L. Xu, Z. Yan, E. Zaccarelli and especially S. Sastry for helpful discussions and the NSF Chemistry Program for support. We also thank the Boston University Computation Center and Yeshiva University for allocation of computational time.

-
- [1] Waller, R., trans. *Essays of natural experiments* [original in Italian by the Secretary of the Academie del Cimento]. Facsimile of 1684 English translation (Johnson Reprint Corporation, New York, 1964).
 - [2] Mishima, O. & Stanley, H. E. (1998) *Nature* **392**, 164–168.
 - [3] Debenedetti, P. G. & Stanley, H. E. (2003) *Physics Today* **56** [6], 40–46.
 - [4] Debenedetti, P. G. (2003) *J. Phys.: Condens. Matter* **15**, R1669–R1726.
 - [5] Angell, C. A. (2004) *Ann. Rev. Phys. Chem.* **55**, 559–583.
 - [6] <http://www.lsbu.ac.uk/water/anmlies.html>.
 - [7] Poole, P. H., Sciortino, F., Essmann, U. & Stanley, H. E. (1992) *Nature* **360**, 324–328.
 - [8] Chen, S.-H., Mallamace, F., Mou, C.-Y., Broccio, M., Corsaro, C., Faraone, A. & Liu, L.

- (2006) *Proc. Natl. Acad. Sci. USA* **103**, 12974–12978.
- [9] Prielmeier, F. X., Lang, E. W., Speedy, R. J. & Lüdemann, H. D. (1987) *Phys. Rev. Lett.* **59**, 1128–1131.
- [10] Egelstaff, P. A., *An Introduction to the Liquid State* (Clarendon Press, New York, 1994).
- [11] Jonas, J. & Akai, J. A. (1977) *J. Phys. Chem.* **66**, 4946–4950.
- [12] Keyes, T. & Oppenheim, I. (1973) *Phys. Rev. A* **8**, 937–949.
- [13] Sillescu, H. (1999) *J. Non-Cryst. Solids* **243**, 81–108.
- [14] Cicerone, M. T., Blackburn, F. R. & Ediger, M. D. (1995) *Macromolecules* **28**, 8224–8232.
- [15] Cicerone, M. T. & Ediger, M. D. (1995) *J. Chem. Phys.* **103**, 5683–5692.
- [16] Berthier, L., Biroli, G., Bouchaud, J.-P., Cipeletti, L., Masri, D. El, L’Hote, D., Ladieu, D. & Pierno, M. (2005) *Science* **310**, 1797–1800.
- [17] Pollack, G. L. (1981) *Phys. Rev. A* **23**, 2660.
- [18] Pollack, G. L. & Enyeart, J. J. (1985) *Phys. Rev. A* **31**, 980.
- [19] Ediger, M. D. (2005) *Annu. Rev. Phys. Chem.* **51**, 99–128.
- [20] Fujara, F., Geil, B., Sillescu, H., & Fleischer, G., (1992) *Z. Phys. B* **88**, 195–204.
- [21] Cicerone, M. T., Blackburn, F. R. & Ediger, M. D. (2005) *J. Chem. Phys.* **102**, 471–479.
- [22] Ehlich, D. & Sillescu, H. (1990) *Macromolecules* **23**, 1600.
- [23] Starr, F. W., Angell, A., Stanley, H. E. (2003) *Physica A* **323**, 51–66.
- [24] Stillinger, F. H. & Hodgson, J. A. (1994) *Phys. Rev. E* **50**, 2064.
- [25] Gilles, T. & Kivelson, D. (1995) *J. Chem. Phys.* **103**, 3071–3073.
- [26] Ngai, K. L. (1999) *Phil. Mag. B* **79**, 1783–1797.
- [27] Weeks, E. R., Crocker, J. C., Levitt, A. C., Schofield, A., Weitz, D. A., (2000) *Science* **287**, 627–631.
- [28] Kanno H. & Angell, C. A., (1979) *J. Chem. Phys.* **70**, 4008–4016.
- [29] Starr, F. W., Sciortino, F., Stanley, H. E., (1999) *Phys. Rev. E* **60** 6757–6768.
- [30] Rössler, E., (1990) *Phys. Rev. Lett.*, 1595–1598.
- [31] Mahoney, M. W & Jorgensen, W. L. (2000) *J. Chem. Phys.* **112**, 8910–8922.
- [32] Yamada, M., Mossa, S., Stanley, H. E. & Sciortino, F. (2002) *Phys. Rev. Lett.* **88**, 195701.
- [33] Paschek, D. (2005) *Phys. Rev. Lett.* **94**, 217802.
- [34] Stillinger, F. H. & Rahman, A. (1974) *J. Chem. Phys.* **60**, 1545.
- [35] Becker, S. R., Poole, P. H. & Starr, F. W. (2006) *Phys. Rev. Lett.* **97**, 055901.

- [36] Poole, P. H., Saika-Voivod, I. & Sciortino, F. (2005) *J. Phys.: Condens. Matter* **17**, L431–L437.
- [37] The experimental data for D were taken from Ref. [9] and the experimental data for η were taken from Ref. [38]. The T_W for experimental water at $P = 1$ atm is taken to be 225 K [46] which is also supported by simulation studies of the SPC/E model of water [23].
- [38] Hallet, J. (1963) *Proc. Phys. Soc.* **82**, 1046–1050; Opisov, Y. A., Zheleznyi, B. V., & Bondarenko, N. F. (1977) *J. Phys. Chem.* **51**, 748–752; Angell, A. (1981) in *Water: A comprehensive treatise*, edited by F. Franks (Plenum press, New York).
- [39] Starr, F. W., Harrington, S., Sciortino, F. & Stanley, H. E. (1999) *Phys. Rev. Lett.* **82**, 3629–3632.
- [40] Donati, C. *et al.* (1999) *Phys. Rev. E* **60**, 3107–3119.
- [41] Giovambattista, N., Buldyrev, S. V., Stanley, H. E. & Starr, F. W. (2005) *Physical Review E* **72**, 011202.
- [42] Tsai K. H., & Wu T.-M., (2005) *Chem. Phys. Lett.* **417**, 390–395.
- [43] Errington J. R. & Debenedetti P.G, (2001) *Nature* **409**, 318–321.
- [44] Kumar, P., Yan Z., Xu, L., Mazza, M, Buldyrev, S. V., Chen, S.-H., Sastry, S. & Stanley, H. E., (2006) *Phys. Rev. Lett.* **97** , 177802.
- [45] Xu, L., Kumar, P., Buldyrev, S. V., Chen, S.-H., Poole, P. H., Sciortino, F. & Stanley, H. E., (2005) *Proc. Nat. Acad. Sci.* **102** 16558–16562.
- [46] Maruyama, S., Wakabayashi, K. & Oguni, M. (2004) *AIP Conf. Proc.* **708**, 675–676.
- [47] Kumar, P., Buldyrev, S. V., Stanley, H. E., (2007) (to be submitted).
- [48] Kumar, P., Franzese, G., and Stanley, H. E., (submitted Dec 06).
- [49] Liu, L., Chen, S.-H., Faraone, A., Yen, C.-W & Mou, C.-Y (2005) *Phys. Rev. Lett.* **95**, 117802.
- [50] Mallamace F., Broccio M., Corsaro C., Faraone A., Wanderlingh U., Liu L., Mou, C.-Y., & Chen, S.-H. (2006) *J. Chem. Phys.* **124**, 161102.

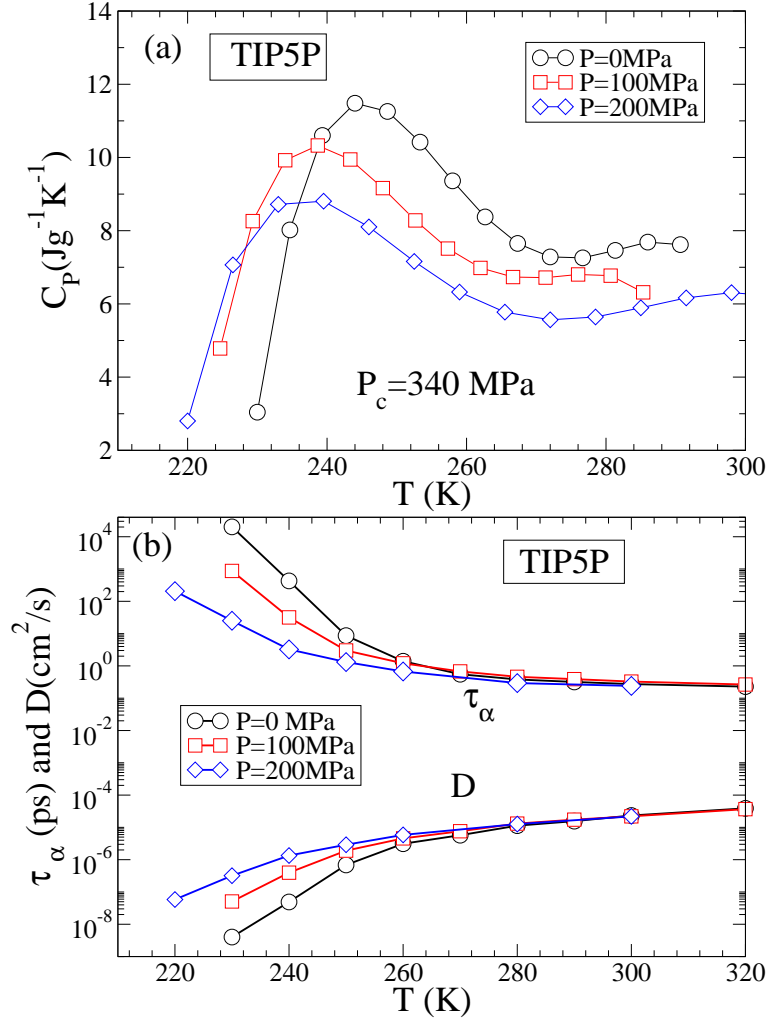


FIG. 1: Temperature dependence of (a) C_P and (b) τ_α and D for $P = 0$ MPa, 100 MPa and 200 MPa. We note that while the temperature of the maximum decreases with pressure, the value of $C_P(T)$ at the maximum also decreases. This could be an artifact of the TIP5P potential which is known not to correctly reproduce the radial distribution function at high pressures.

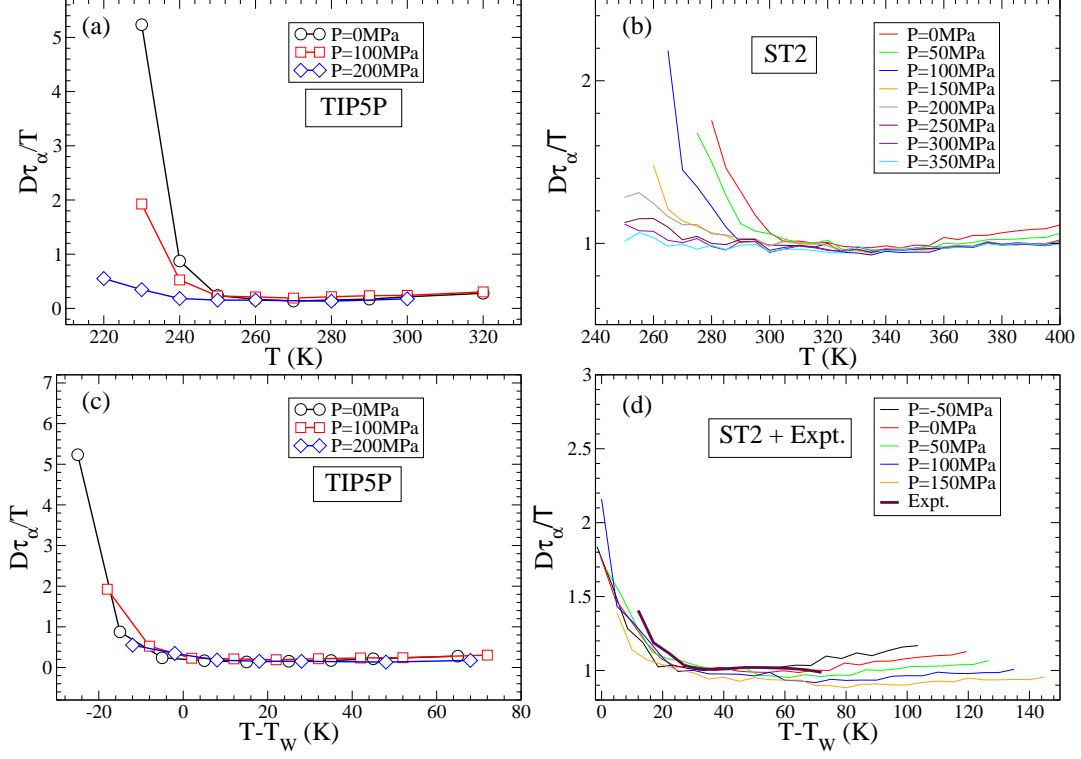


FIG. 2: (a) $D\tau_\alpha/T$ as a function of T for $P = 0$ MPa, 100 MPa and 200 MPa for the TIP5P model. For all panels, $D\tau_\alpha/T$ is scaled by its high T value to facilitate comparison of the different systems. (b) Analog of Fig. 2(a) for the ST2 model. (c) $D\tau_\alpha/T$ as a function of $T - T_W(P)$ for TIP5P. (d) Analog of Fig. 2 (c) for the ST2 model including the experimental curve of $D\eta/T$ for water.

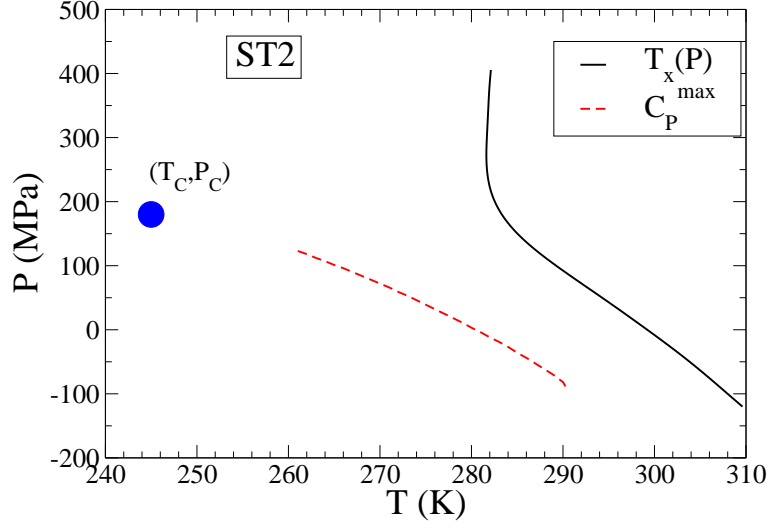


FIG. 3: Locus in P-T plane of C_P^{max} and $T_x(P)$ for the ST2 model. Filled circle denotes the liquid-liquid critical point (T_C, P_C) in ST2 model.

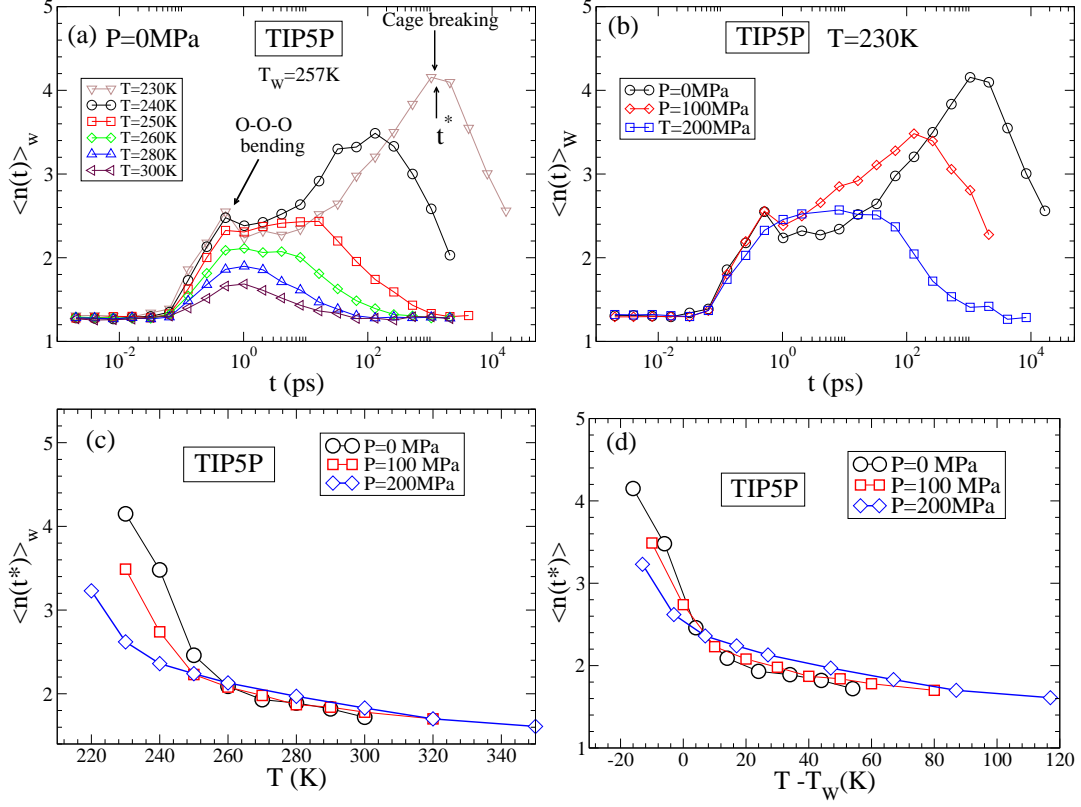


FIG. 4: Mobile particle cluster size $\langle n(t) \rangle_w$ (a) for different T at $P = 0$ MPa and (b) for different P at $T = 230$ K. (c) $\langle n(t^*) \rangle_w$ for $P = 0$ MPa, 100 MPa and 200 MPa. (d) $\langle n(t^*) \rangle_w$ as a function of $T - T_w(P)$ for three different P . All these plots are for the TIP5P model.

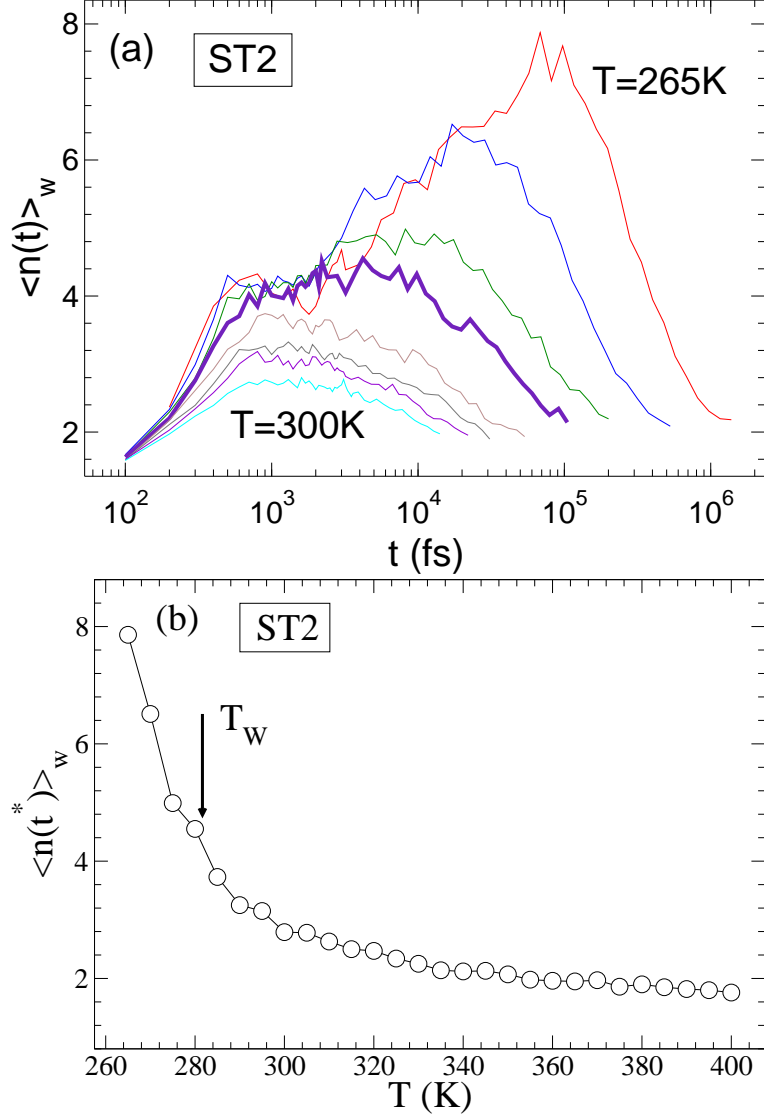


FIG. 5: Dynamical heterogeneities in the ST2 model of water. (a) $\langle n(t) \rangle_w$ as a function of t at 5 K intervals for $\rho = 0.83 \text{ g/cm}^3$ from 265 K to 300 K. The bold line shows the $T = 280 \text{ K}$ isotherm where the constant volume specific heat C_V has a maximum. (b) $\langle n(t^*) \rangle_w$ as a function of T for $\rho = 0.83 \text{ g/cm}^3$. We indicate the temperature at which C_V has a maximum by a vertical arrow. The maximum of C_V occurs in the same region where other response functions, such as C_P , have maxima.

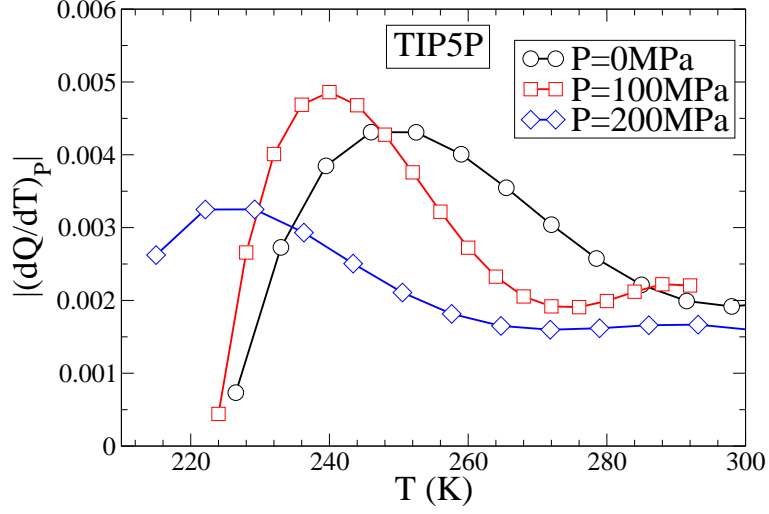


FIG. 6: $|(\partial Q/\partial T)_P|$ as a function of T for $P = 0$ MPa and 100 MPa and 200 MPa. We note that while the temperature of the maximum decreases with pressure, the value $|(\partial Q/\partial T)_P|$ at the maximum for $P = 200$ MPa than the lower pressures. This could be an artifact of the TIP5P potential which is known not to correctly reproduce the radial distribution function at high pressures.